REPORT DOCUMENTATION PAGE

DTIC ELECTE MAY 06 1994 S G D

1a. REPORT SECURITY CLASSIFICATION: unclassified	1b. RESTRICTIVE MARKINGS: none
2a. SECURITY CLASSIFICATION AUTHORITY	3. DISTRIBUTION / AVAILABILITY OF REPORT: DISTRIBUTION UNLIMITED
2b. AD-A278 966	
4.	5. MONITORING ORGANIZATION REPORT NUMBER(S)
6a. NAME OF PERFORMING ORGANIZATION: Aerospace & Energetics Research Program, FL-10 / 6b. OFFICE SYMBOL (If applicable): 12104	7a. NAME OF MONITORING ORGANIZATION: Office of Naval Research U of W Resident Representative N63374
6c. ADDRESS (City, State, and ZIP Code): Grant & Contract Services, JM-24 University of Washington Seattle, WA 98195	7b. ADDRESS (City, State, and ZIP Code): University of Washington 1107 NE 45th St, Univ Dist Bldg Rm 410 Seattle, WA 98105-4631
8a. NAME OF FUNDING / SPONSORING ORGANIZATION: Office of Naval Research / 8b. OFFICE SYMBOL (If applicable): 1262	9. PROCUREMENT INSTRUMENT IDENTIFICATION NUMBER: N00014-90-J-1676
8c. ADDRESS (City, State, and ZIP Code): 800 North Quincy Street Arlington, Virginia 22217-5000	10. SOURCE OF FUNDING NUMBERS: PROGRAM ELEMENT NO. / PROJECT NO. / TASK NO. / WORK UNIT ACCESSION NO.

11. TITLE (Include Security Classification)
"Gas Optics Applicable to Free Electron Laser Technology"

94-13760

12. PERSONAL AUTHOR(S)
CHRISTIANSEN, Walter Henry

13a. TYPE OF REPORT	13b. TIME COVERED	14. DATE OF REPORT
final technical report	FROM 90/1/1 TO 91/7/15	

16. SUPPLEMENTARY NOTATION

17. COSATI CODES		
FIELD	GROUP	SUB-GROUP

18. SUBJECT TERMS (Continue on reverse if necessary and identify by block number)
gas optics; free electron lasers; aerodynamic windows

19. ABSTRACT (Continue on reverse if necessary and identify by block number)

The mass flow characteristics and optical qualities of axisymmetric free-jet aero-windows with passively induced swirl were studied for applications to free electron lasers. The aero-windows considered are axial supersonic flows from free-jets of various sizes. Mass flow rates through the nozzles are measured and compared to measured non-swirled flow rates and theoretical values. The effect of nozzle size on swirl induction is studied. Optical qualities are measured in the far field in the laboratory and compared with optical measurements from the non-swirled cases. The optical results for swirling flow shows weak defocusing and good Strehl ratios in contrast to focusing effects and good Strehl ratios for non-swirled flow.

421 049

20. DISTRIBUTION / AVAILABILITY OF ABSTRACT	21. ABSTRACT SECURITY CLASSIFICATION
☐ UNCLASSIFIED/UNLIMITED ☒ SAME AS RPT. ☐ DTIC USERS	
22a. NAME OF RESPONSIBLE INDIVIDUAL: Donald W. Allen	22b. TELEPHONE (Include Area Code): (206) 543-4043 / 22c. OFFICE SYMBOL: 12104

DD FORM 1473, 84 MAR — 83 APR edition may be used until exhausted. All other editions are obsolete.

SECURITY CLASSIFICATION OF THIS PAGE
unclassified

94 5 05 204

GAS OPTICS APPLICABLE TO FREE ELECTRON LASER TECHNOLOGY

Final Technical Report 1991

Contract N00014-90-J-1676

I. Introduction

The research and development of lasers such as free electron lasers (FEL's) have stimulated the need for the development of a new class of optics. These optics must be able to withstand enormous light intensities while maintaining consistently high optical performance. Gas dynamic optics which use the refractive index change occurring in compressible and non-isothermal gas flows can be used to satisfy these requirements. Gas optics continuously replace themselves with new material via the flow process thereby avoiding many possible problems associated with material breakdown.

One gas optical system currently being proposed for the FEL uses a defocusing thermal gradient gas lens. This gas lens will operate at atmospheric pressure while the FEL wiggler cavity must be maintained at pressures less than 10^{-8} atm. Some sort of aero-window device must be used at the interface between the wiggler cavity and the thermal lens.

Any aero-window used for the vacuum interface must have two important features: first, it must act as a high-quality optical element (it must not degrade the laser beam), and second, it should minimize the mass flow from the thermal lens system into the wiggler cavity. Recent research [1] has been conducted analyzing the mass flow characteristics and the optical performance of a simple axisymmetric aero-window. These results indicated high Strehl ratios with weak Fresnel focusing, and predictable, but high, mass flow rates.

Tangential swirling was suggested in ref. [1] as a method for mass flow reduction and weakening the focusing effect. This investigation considers the mass flow characteristics and the optical performance of an axisymmetric aero-window with passively induced swirl. (i.e. swirl induced into the flow field using stationary turning vanes.)

II. Past Work on the Vacuum Interface Experiment

Mass flow measurements without swirls have been completed for various nozzles, and Strehl ratios have experimentally been shown to be high. In addition, analysis has indicated that the pumping power requirements for cw operation, while large, may be lower than previously expected. The main apparatus consists of a 2.7 m^3 vacuum tank equipped with mechanical pumps and one diffusion pump. On opposing sides of the tank are a laser window and the vacuum interface as shown in Fig. 1.

Accesion For	
NTIS CRA&I	☒
DTIC TAB	☐
Unannounced	☐
Justification	
By	
Distribution /	
Availability Codes	
Dist	Avail and / or Special
A-1	

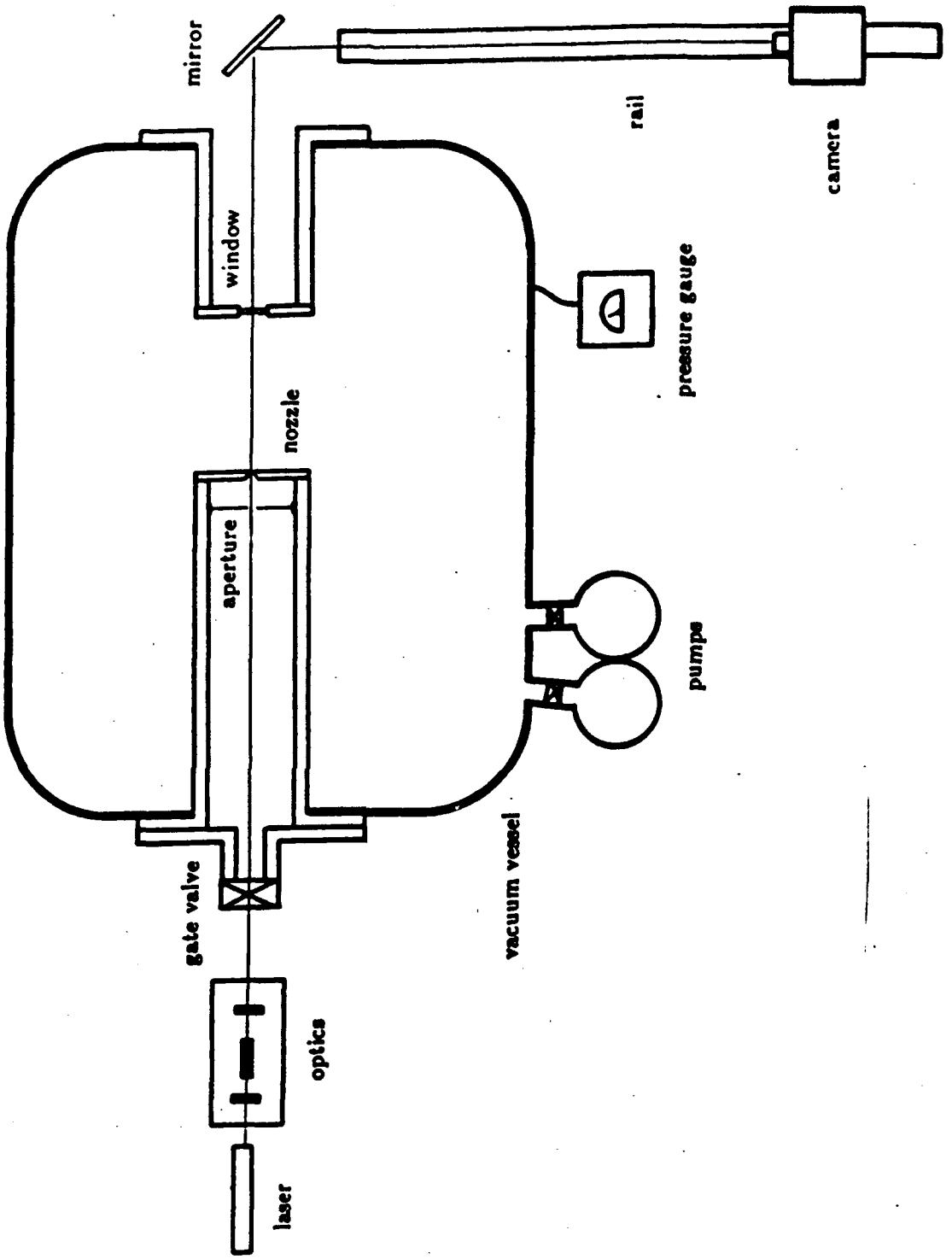

Figure 1: The laboratory apparatus

The laser source is a HeNe laser which is spatially filtered, columnated, and masked to a final diameter of between 2.5 mm to 5 mm. The beam is aligned with the axis of the orifice. With the laser beam aligned, a gate valve (which is external to the orifice) is closed and the tank is evacuated. Upon opening the valve, a free jet flow occurs at the orifice. The laser beam (which is in the near field at the location of the orifice) is then optically perturbed by the flow. The far field pattern is imaged and detected with a digital camera and recorded to computer memory. The recorded information can then be manipulated thereby determining Strehl ratio and focus effects.

The numerical predictions for large focal lengths indicated the aerowindows would act as low Fresnel number lenses, thus a low Fresnel number reference system was used for the laboratory experiment. The intensity distributions measured were found to agree very well with the theoretical distributions. The experimental results for focal length matched the numerical ones quite well. Focal lengths varied from 9-21 m for nozzle diameters ranging from 3.58-8.33 mm respectively. A sharp-edged orifice produced a focal length shorter than a smooth nozzle with the same diameter. Focal lengths increased slightly with increasing beam size at fixed nozzle diameter.

Focus-corrected Strehl ratios were very high--ranging from 1.0 for the smallest nozzle to .96 for the largest nozzle. The flow fields were solved numerically and the Zernike aberration coefficients determined. The most complete description of this work is given in Ref. 1.

III. Current Aerowindow with Swirl to Vacuum Experiments.

A. Background and Analysis

Swirl was added to the axial flow of a nozzle flow to see the effects that this motion has on mass flow rate and the optimal quality. The most direct method of passively inducing a tangential flow component is the use of turning vanes. Turning vanes can alter the vector direction of the flow while maintaining constant enthalpy (h_o = const) and without requiring any exterior control. The proper design of a turning vane device to induce large amounts of tangential flow was developed.

To take maximum advantage of the conservation of angular momentum the turning vanes should be located radially as far from the axis as possible. A flow director will then be required to ensure that all the flow enters the turning vanes. The blade angle of the turning vanes can be determined knowing the ratio of nozzle area to turning vane area, the ratio of nozzle radius to turning vane radius, the density ratio, and the desired tangential velocity at the nozzle. A converging throat section after the turning vanes will then constrict the channel radius and induce the increase in tangential velocity as the flow approaches the throat. In addition a conical flow guide can be used after the turning vanes. Figure 2 shows a schematic diagram of a swirl induction device and its accompanying parts.

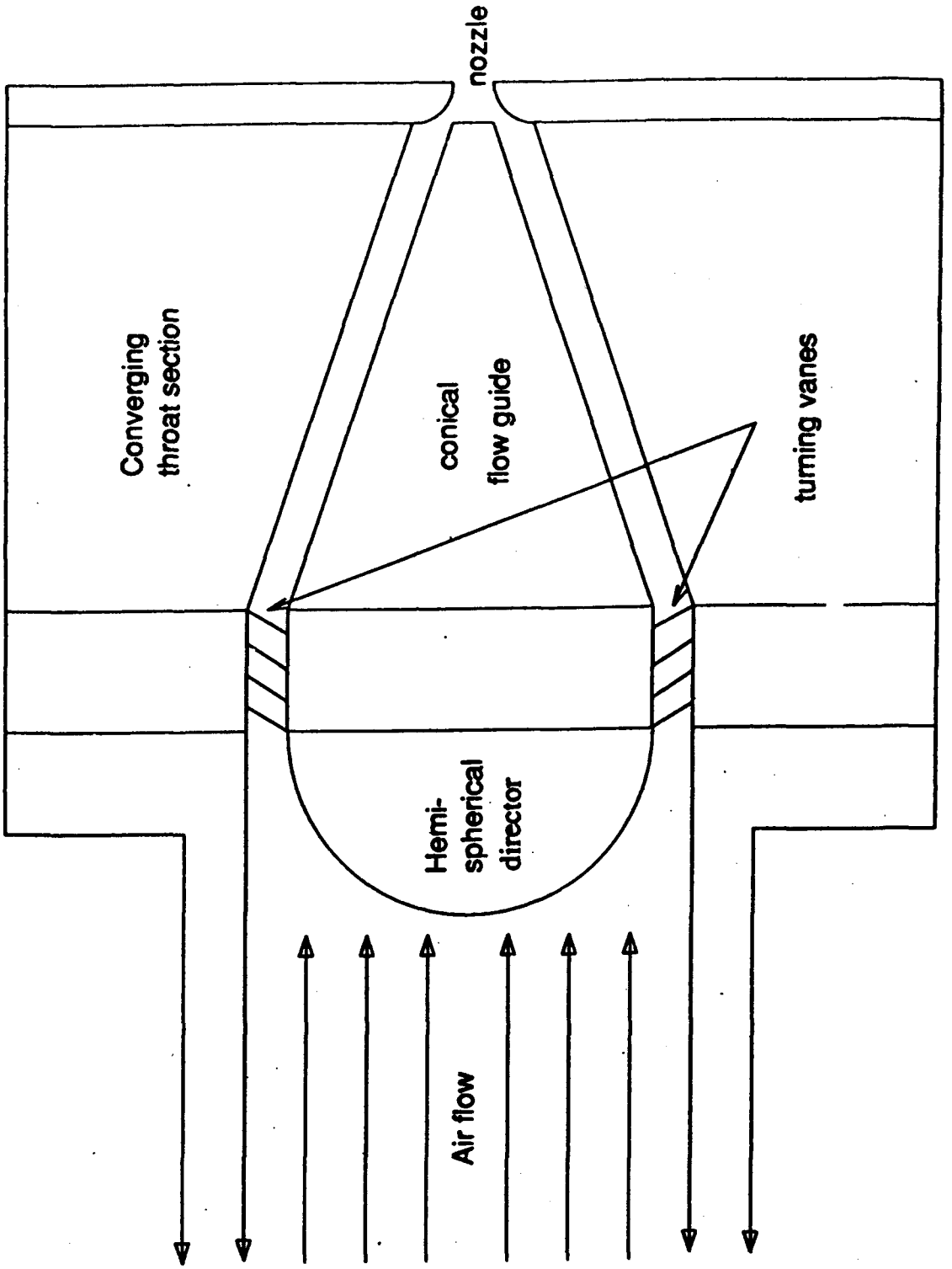

Figure 2: Swirl induction schematic diagram

Numerical predictions provided theoretical values for the mass flow reduction which could be compared to laboratory data. For the numerical calculations, the radial velocity field was assumed to approximate a solid body rotation. Additionally the fluid in question was assumed to be air. (Υ = 1.4). With these assumptions the reduced mass flow becomes

$$\Gamma \frac{(\text{mass flow rate w swirl})}{(\text{mass flow rate wo swirl})} = \frac{1}{4\Omega^2}\left[1-(1-\Omega^2)^4\right]$$

Where Ω is the non-dimensional rotation rate, the tangential speed divided by $\sqrt{\frac{2}{\gamma-1}}\, a_0$ (stagnation speed of sound). The values of Ω were calculated in a multi-step process involving the area and radius ratio of the nozzle and turning vane cross section, the density ratio, and the chosen blade angle. All flow velocities were originally non-dimensionalized by the speed of sound at the throat.

The experimental aero-windows nozzles used were three smooth, quarter radius contoured nozzles. The three smooth nozzles were identical except for their throat diameters (d=3.58, 5.04, and 8.33 mm). Each nozzle had a smooth, quarter radius contour ending at the throat which was intended to produce a straight sonic line at the throat. The results of the numerical calculations for the specific nozzles used in the experiment are shown in table 1. The details of the calculations and description of the apparatus can be found in ref. 2.

Table 1 Theoretical mass flow ratios, Γ

Nozzle diameter	3.58 mm	5.04 mm	8.33 mm
Mass flow ratio $\theta = 25°$	0.900	0.833	0.701
Mass flow ratio $\theta = 30°$	0.928	0.877	0.762

The slightly modified vacuum interface apparatus used in the laboratory is shown schematically in figure 3. It consisted of interchangeable nozzle plates attached to a port on a large vacuum tank. One 750 1/s cold trapped diffusion pump provided the evacuation to the $3.35m^3$ tank. The laser and all optics were located outside the tank. A large rubber stopper provided vacuum integrity while sealed and permitted rapid manual opening and closing to allow air flow into the tank. The swirl induction device was located in an intruding 102 mm I.D. aluminum tube extending into the tank, directly before a converging throat section leading to the nozzle. Nozzle plates were bolted to the end of the aluminum tube inside the tank. The intruding tube was fitted with an aluminum insert restricting the flow area to a 50.4 mm diameter cross section. The optical window was fastened to a similar tube extending into the tank from the opposite side. The laser beam was carefully aligned to pass through the swirl inducer, the center of the nozzle and exit the tank through the window. A CCD camera was located outside the tank, mounted on a traversing rail.

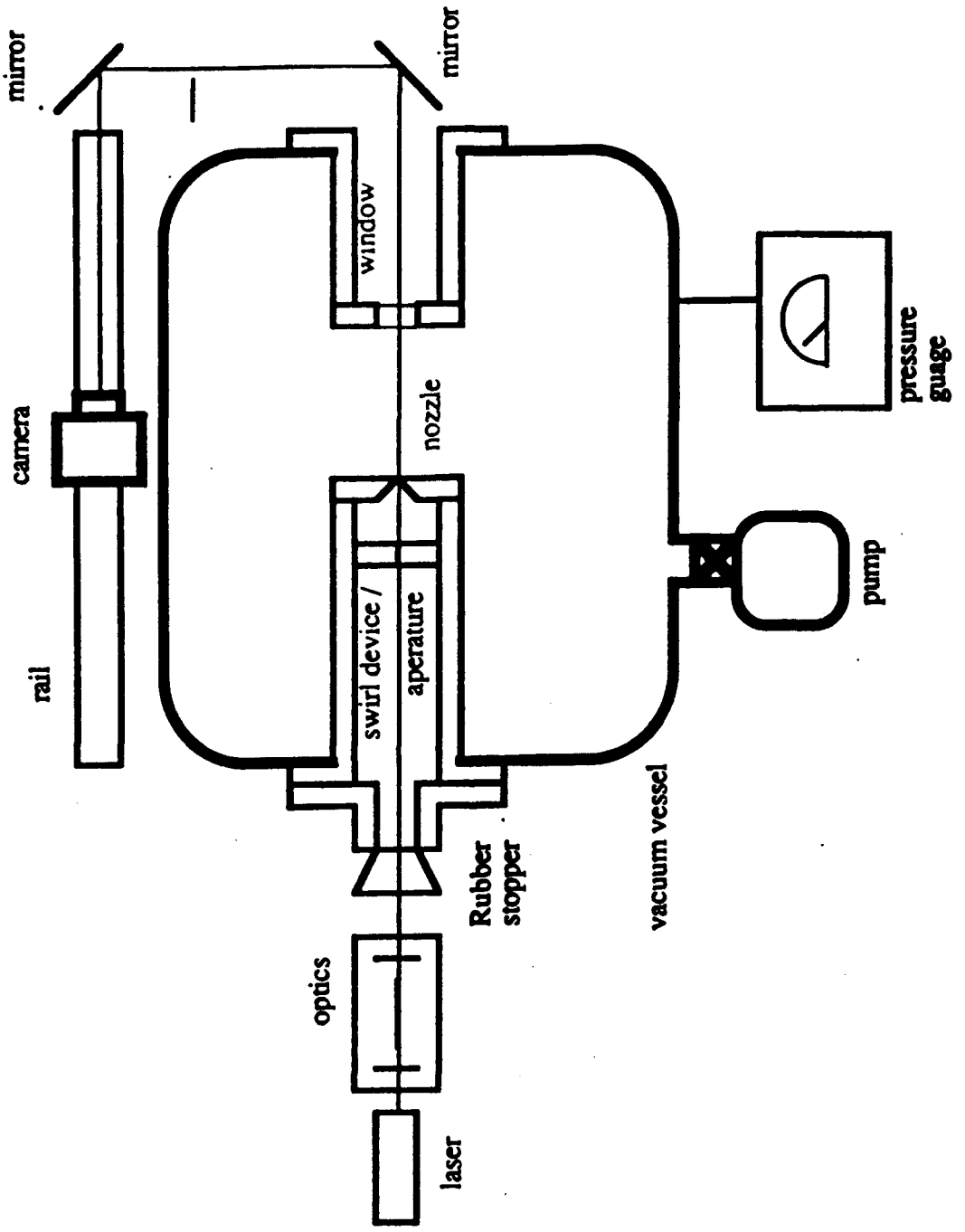

Figure 3: The laboratory apparatus

B. Measurements

The results from the mass flow measurements are shown in table 2. The nozzles produced mass flow rates 4.3%, 3.7%, and 12.1% less than one-dimensional theoretical values for the 3.58 mm, 5.04 mm, and 8.33 mm nozzles respectively for the un-swirled case. The 6 bladed swirled case produced mass flow rates 18.8%, 31.2 %, and 55.4% less than the non-swirled values for the 3.58 mm, 5.04 mm, and 8.33 mm nozzles respectively. Repeated measurements of the tank volume varied about $\pm$2.0%. This error transfers directly to the mass flow rates and could account for some of the deviation from theory. The assumption of true one-dimensional flow can also be questioned, but was made for simplicity.

Table 2: The swirl mass flow ratios

	Straight flow	Swirled flow 6 bladed	Swirled flow 8 bladed	Swirled flow 6 bladed with hole
Nozzle	Γ	Γ	Γ	Γ
3.58 mm	1.0	0.848	0.933	0.922
5.04 mm	1.0	0.714	0.749	0.836
8.66 mm	1.0	0.507	0.523	0.589

The results of the optical measurements are shown in tables 3 and 4. The spot radius was measured in camera pixels (58 pixels / mm) from maximum count to the background count. The observed spot radius with swirl was consistently larger than the tare spot radius, while the ratio of swirl spot radius to tare spot radius remained approximately constant for varying camera distances. This suggests that the swirl produced additional beam spreading proportional to the natural Airy spread angle of the laser through air. Defining α as the half angle of beam spread we obtain.

Table 3: Maximum radius of Tare and Swirl spot sizes in # of pixels

	Tare	Swirl	Ratio: swirl/tare
Test #	radius	radius	
1	102	111	1.088
2	103	114	1.107
3	104	111	1.067
4	100	110	1.100
Average	102.25	111.5	1.088

$$\alpha_{swirl} = .0878\alpha_{Airy} \qquad \text{with} \qquad \alpha_{Airy} = \frac{1.22\lambda}{D}$$

For $\lambda = 6.33 \times 10^{-7}$m and D = beam aperture diameter =.001 m this corresponds to $\alpha_{swirl} = .678 \times 10^{-4}$ rad. The value of α_{swirl} is probably accurate to within ± 10%. This error is due to the laser output variations as well as uncertainty in camera resolution. Calculating the corresponding focal point for this spread angle and the given beam diameter using

$$f = -\frac{D/2}{\text{Tan}(\alpha_{swirl})}$$

leads to a focus at approximately -7.4 m. The focal length is probably accurate to within ±10%. The error in focal length can be inferred from the above equation.

Table 4 shows the single shot and time average values of the peak intensities of the optical data for swirling flow and the corresponding no flow tar measurements. The Strehl ratios for the straight flow and corresponding tare measurements are not shown but strongly agreed with the results of previous work [1]. The computed Strehl ratios without focus correction were all consistently low compared to previous values obtained for the straight flow case. They ranged from approximately 0.829 to 0.867 and averaged 0.847, however, when

correcting for the defocusing effects Strehl ratios of 1.0 were achieved to within experimental tolerance limits.

Table 4: Tare and swirl peak intensities

	Tare	Swirl	Ratio	Focus corrected
Test #	I_o	I_o	(swirl/tare)	Strehl ratio
1	189	161	.85185	1.008
2	190	159	.83684	1.025
3	187	162	.86631	0.986
4	186	155	.83333	1.008
Average	188	159.25	.84707	1.003

IV. Summary

Measured mass flow rates with swirl were in all cases lower than predicted by theory. The 5.04 and 8.33 mm nozzles demonstrated a 28.6% and 49.3% mass flow reduction respectively over 1-dimensional choked flow, while the 3.58 mm nozzle demonstrated a 15.2% reduction over 1-D choked flow.

The numerical analysis of the optical data indicated the aero-window acted as a weakly defocusing optical element with an extremely high focus corrected Strehl ratio. The defocus corresponded to an 8% increase in spread angle over the natural diffraction spread angle, corresponding to a focus at approximately -7.4 m for 1mm diameter beam in air.

The intensity distribution measurements were obtained from time averaged digitized pictures of the beam spot. Strehl ratios were obtained from numerical integration and comparison of swirling flow data to tare data. The numerical results indicated Strehl ratios ranging from 0.829 to 0.867 and averaging 0.847 without focus correction, and Strehl ratios of 1, within experimental tolerance limits, with focus correction.

References

1. Meyer, Perry A., M.S. Thesis 1988, "The Axisymmetric Free-Jet as an Aero-Window", Department of Aeronautics and Astronautics, University of Washington.

2. Gurevich, Peter A., M.S. Thesis 1992, "Swirl Effects on the Axisymmetric Free-Jet as an Aero-Optical Window", Department of Aeronautics and Astronautics, University of Washington.